



Preparation and properties of novel flame-retardant PBS wood-plastic composites

ShuaiCheng Jiang^{a,1}, YaFeng Yang^{b,1}, ShengBo Ge^a, ZhongFeng Zhang^{a,*},
WanXi Peng^{a,b,*}

^a School of Materials Science and Engineering, Central South University of Forestry and Technology, Changsha 410004, China

^b School of Forestry, Henan Agricultural University, Zhengzhou 450002, China

Received 1 September 2017; accepted 21 December 2017

Available online 29 December 2017

KEYWORDS

Poly (butylene succinate);
Crystallization behavior;
Flame retardant;
AHP;
APP;
CaHP

Abstract Poly (butylene succinate) (PBS), as a fully biodegradable thermoplastic, have developed rapidly due to its integrated performance and processibility. The CaCO₃ as a reinforcing component, and AHP, APP and CaHP as a flame-retardant component were separately incorporated into PBS matrix. A series of PBS-based composites were fabricated via melting blending using internal mixer followed by injection molding. The results show that the different filling ratio has a certain influence on the mechanical properties of the composites. When the filling amount of wood powder is 40 copies, the composite mechanical properties of the composite is better. CaCO₃ addition, the composite material of the bending strength, tensile strength have improved significantly. The results showed that small amount of AHP, APP and CaHP improved the tensile strength of PBS composites, however, the tensile strength decreased as further increase amount of AHP, APP and CaHP. Cone Calorimeter testing revealed that, the combination of AHP, APP and CaHP could significantly reduce the pHRR and the total heart release (THR) of the composites. TGA test indicated that the addition of AHP, APP and CaHP could significantly increase the char residue and reduce the mass loss rate. TGA test indicated that the addition of AHP, APP and CaHP could significantly increase the char residue and reduce the mass loss rate. Through the research of mechanical and thermal properties of PBS composite, it could lay a foundation of the application of PBS composite in different fields.

© 2017 The Authors. Production and hosting by Elsevier B.V. on behalf of King Saud University. This is an open access article under the CC BY-NC-ND license (<http://creativecommons.org/licenses/by-nc-nd/4.0/>).

1. Introduction

Facing the coming energy crisis, the world recognized the need to adopt expenditure strategy, on the one hand, energy saving, on the other hand, the development of new energy. In the case of the petrochemical industry, we must find a new way for the synthesis of polymer materials, in order to reduce dependence on oil and other nonrenewable resources. On the other hand, with the development of the times, the shortage of natural

* Corresponding authors at: School of Forestry, Henan Agricultural University, Zhengzhou 450002, China (W. Peng).

E-mail address: pengwanxi@163.com (W. Peng).

¹ Co-first coauthors: Shuaicheng Jiang and Yafeng Yang.

Peer review under responsibility of King Saud University.



Production and hosting by Elsevier

wood has become one of the important problems facing the world today. Governments are working to protect natural resources and strengthening the implementation of forest protection laws. In particular, the rapid development of living conditions, environmental awareness gradually increased.

Plastic was once known as the 20th century's most significant invention. It has been widely used in many fields because of its many excellent performances. The application of plastic products brings great convenience to people, but also brings serious negative effects. Most of the abandoned plastic product, except in the special conditions can be solved. Waste plastics in the natural environment of light, biodegradation rate is very slow, it may take hundreds of years to completely disappear. With the increasing of the plastic dosage, waste plastics are becoming more and more polluted to the environment. The "white pollution" caused by plastics has become a public nuisance worldwide. In order to solve this problem, The research and development of biodegradable plastics is an ideal way to solve white pollution. Biodegradable plastics can be completely decomposed under natural conditions after disposal, and the pollution to the environment is very small. Plastic degradation process refers to the composition of plastic macromolecular chain in the role of light and micro-organisms were cut into small molecules process, it can be broken down into CO₂ and H₂O, eventually disappearing into the natural world (Rath et al., 2012; Sukor et al., 2017; Ismail and Hanafiah, 2017). There are two main types of biodegradable plastics, one is photodegradable plastic, the other is biodegradable plastic (Kutlaková et al., 2011; Halim et al., 2017). Degradable plastics can not only solve the problem of white pollution, but also become an effective way to achieve recycling of resources, which can significantly improve social and economic benefits (Prasannalakshmi et al., 2015; Basheer et al., 2017; Razali and Said, 2017).

Today, sustainable development is the ideal model for global common pursuit, as an important factor in sustainable development, green environmental protection has become a popular topic in the 21st century. The development and application of degradable plastics is an effective way to solve the environmental problems caused by refractory plastic waste. It plays an important role in promoting the development of green environment in the 21st century (Hassan et al., 2017). And the degradable plastics are not only important for green environmental protection, but they can also help alleviate the problem of the current shortage of oil resources. Therefore, it is of great importance to actively develop and utilize biodegradable plastics for environmental protection and the sustainable development of composite materials. These green composites have been widely used in packaging, gardening, automotive, biomedical and other aspects (Mantia and Morreale, 2011; Koronis et al., 2013; Zini and Scandola, 2011; Dicker et al., 2014; Halim and Phang, 2017).

Poly (butylene succinate), PBS, is obtained by condensation of succinic acid and butanediol, the chemical structure is shown in Figs. 1 and 2, The synthesis method consists of two stages: First at the lower reaction temperature, the dibasic acid is reacted with an excess of the diol to form a terminal hydroxyl group prepolymer, And then remove the diol to obtain the polyester in high temperature, high vacuum and catalyst conditions. PBS is a non-toxic white particle, a semi-crystalline polymer. PBS, Density: 1.27 g/cm³, Melting point: 114 °C, Decomposition temperature: 300 °C, Glass transition

temperature: -32 °C, Crystallinity: 30-60%, Crystallinity temperature: 75 °C. PBS is a fully biodegradable polymer material, has good biological compatibility and biological absorbability (Shamsudin et al., 2017). PBS, Under the catalysis of bacteria or enzymes, can eventually be degraded to non-toxic and harmless substances such as carbon dioxide and water [4-7]. The degradation is due to the breakage of chemical bonds in the polymer, including the breakage of chemical bonds in the main chain and the branch, in which the degradation of the polymer plays a decisive role in the cleavage of the main chemical bonds. As a new biodegradable polymer material, PBS has developed rapidly and has attracted much attention because of its good thermal stability and mechanical properties.

With the market demand for degradable materials growing, PBS has expanded its application, because it has better processability and practicality. At present, PBS has been used in the field of packaging, medical and automotive fields (Deschamps et al., 2001; Aziz and Hanafiah, 2017). The cost of PBS is more expensive than traditional nonbiodegradable polymers. It is well known that this shortcoming can be overcome by mixing with cheap natural fibres/fillings (Dash et al., 2008), while maintaining or enhancing the substrate performance.

With the increasingly stringent national energy and environmental regulations and the large-scale development of the PBS molding process, the material cost of PBS is expected to be further reduced. How to combine the advantages of plastic and wood, the development of new environmentally friendly wood materials, has become a major problem people need solve. Therefore, a variety of natural wood are used to fabricate composites with the PBS matrix (Zini and Scandola, 2011), in addition to being inexpensive, natural wood are renewable, sustainable, biodegradable, abundant, and have good specific properties (Gamon et al., 2013; Rahman et al., 2017; Khan et al., 2017). So the new wood plastic composite (WPC) material came into being. It is mixed with lignocellulosic fillers and some thermoplastics (PVC, PP, PE, etc.) as the main raw material (Ayrilmis and Jarusombuti, 2010); With the addition of certain processing aids, the composites were prepared by high temperature mixing and molding. Compared to wood-based panels, the biggest advantage of WPC is non-toxic and environmentally friendly. As a substitute for wood, WPC not only has a unique wood texture, and it has good mechanical properties, good dimensional stability, water resistance, abrasion resistance, excellent chemical resistance, not afraid of insects, easy to color, low maintenance requirements, Long life, easy to shape, can be secondary processing and many other excellent performance. It is also worth mentioning that it can also make full use of recycled wood, spare materials, wood chips and other original waste wood. And it greatly improve the utilization of natural wood, and can solve the waste wood caused by waste pollution and handling problems. It has the function of protecting the natural environment and increasing the added value of artificial wood products. In addition, because the WPC production process using molding, which can be achieved automatically continuous production and the length of arbitrary ruling, while the wood can not. Therefore, WPC has attracted extensive attention in the world, and is regarded as a new type of green environmental protection material, and has broaden prospects for development.

At present, PBS flame retardant mainly uses additive flame retardant and intrinsically flame retardant. Additive flame retardants mainly used to add ammonium polyphosphate as

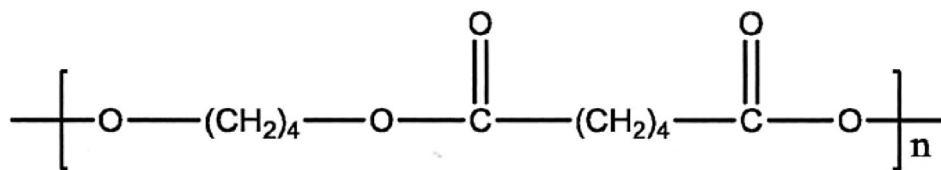


Fig. 1 The chemical structure of the PBS.

the representative of the expansion of flame retardants and a small amount of aluminum hydroxide as the representative of the metal hydroxide flame retardant. Metal hydroxide flame retardants generally require a large amount of added to achieve flame retardant effect, while the high addition of the material will lead to the decline in mechanical properties. And the expansion type of flame retardant usually needs about 30% of the added quantity to achieve the excellent flame retardant effect. At present, hypophosphite is represented by AHP as a novel halogen-free flame retardant. AHP is widely used in engineering plastics polyester and polyamide flame retardant and received good results; So far, there have been few reports of high-efficiency flame retardants such as AHP, CaHP and APP for the flame retardant on PBS. And, PBS and engineering plastics polyester have similar structures. Therefore, a series of hypophosphite flame retardants, such as AHP, used in PBS flame retardant. AHP, CaHP, APP and PBS were mixed to prepare flame retardant PBS/AHP, PBS/CaHP and PBS/APP composites, in order to obtain a good flame retardant effect.

At present, the research on the thermal resistance of new polymer materials, especially flame-retardant polymer composites, has been extensively studied and made at home and abroad. In the actual fire, the non-thermal hazard of the polymer fire is mainly from the narcotic gases that are released during combustion, Such as CO and HCN, irritant harmful gases such as aldehydes, halogenated oxygen, sulfide, nitrogen oxides, polycyclic aromatic hydrocarbons and smoke particles; these ingredients will cause physical and psychological problem, which will do harm to the people in the fire, which is the main cause of personal injury in the event of fire (Gann et al., 2010; Yang et al., 2008; Ghafar et al., 2017). Therefore, the industry should pay more attention to the thermal hazard of new polymer materials and strengthen the study of non thermal hazard. This will help reduce the smoke of polymer materials and effectively prevent the occurrence of fire hazards, this also provides a theoretical basis for high-safety polymer materials.

The aim of this study was to prepare wood plastic composite (WPC) under various conditions and study their chemical structure by X-ray diffractometry (XRD), Fourier transform infrared spectroscopy (FT-IR), thermogravimetric analysis (TGA), and thermal desorption-gas chromatography-mass spectrometry (TD-GC-MS).

2. Material and methods

2.1. Experimental materials

Decayed *Pinus massoniana* Lamb. was collected from the Liyang Forest region in south of China. The decayed *Pinus massoniana* Lamb. was dried in air and crushed into 40–80 mesh. The AHP, APP, CaHP and CaCO₃ were obtained from Chemical New Materials Co., Ltd. The PBS was obtained from Zhengzhou All Stroke Chemical Products Co., Ltd.

2.2. Experimental methods

2.2.1. Mold pressing

The wood pieces and lignin were weighed (200 g), mixed, laid over a mold, and pressed at a surface pressure of 8–10 MPa (Table 1). The PBS samples were prepared for the following tests.

2.2.2. Mechanical property analysis

According to the national standard GB/T17657-2013 and GB/T1040.5-2008 to test the physical and mechanical properties.

2.2.3. Cone calorimeter analysis

Cone calorimeter was founded by NIST first successfully developed in the United States, 1982. It can be used to evaluate combustion characteristic of materials (Schartel and Hull, 2010). Cone calorimeter test was carried out according to the ISO5660 standard which the sample size is 100 mm × 100 mm thickness as the original sample thickness.

2.2.4. FT-IR analysis

The FT-IR spectra of the samples were obtained on a FT-IR spectrophotometer (IR100) using KBr discs containing 1.00% finely ground sample (Peng et al., 2014; Xue et al., 2014; Jiang et al., 2017).

2.2.5. TG analysis

Each sample was analyzed using less than 10 mg of powder. TG spectra were measured from room temperature to 700 °C on a TG20 thermal gravimetric analyzer (209-F1 TG, Netzsch, Germany) using a carrier gas (N₂) velocity of 40 mL/min and a heating rate of 10 °C/min.

2.2.6. XRD analysis

After sample preparation, the samples were examined using an XD-2 diffractometer (General Analysis, Beijing General Instrument Co., Ltd., Beijing, China) with Cu radiation (λ 1.5406 nm), voltage of 36 kV, and current of 20 mA. The 2θ range was scanned continuously with a linkage scanning system (rotary half-cone 2θ) from 5° to 60°, at a scanning velocity of 4°/min and a scan step of 0.01°. A graphite crystal monochromator was used, with slit device widths of DS518, SS518, and RS50.3 mm (Peng et al., 2013).

2.2.7. TD-GC-MS analysis

Each samples of 5 g each were placed in the sample tubes of a Master TD thermal desorber (DANI Co., Ltd., Italy), and the sample tubes were purged with 120 °C He for 30 min. The trap adsorption temperature was set to 120 °C, trap resolution temperature to 130 °C, valve temperature to 130 °C, and transmission line temperature to 130 °C. The volatiles were desorbed

Table 1 Optimization of hot-pressing process.

Samples	Decayed wood (%)	PBS (%)	CaCO ₃ (%PBS)	AHP (%PBS)	APP (%PBS)	CaHP (%PBS)
A1	30	70	5			
A2	40	60	5			
A3	50	50	5			
A4	40	60	5	5		
A5	40	60	5	10		
A6	40	60	5	15		
A7	40	60	5		5	
A8	40	60	5		10	
A9	40	60	5		15	
A10	40	60	5			5
A11	40	60	5			10
A12	40	60	5			15
A13	40	60	5	5	5	5
A14	40	60				

Table 2 Hot-pressing process optimization test results.

Samples	Failing load (N)	MOR (MPa)	MOE (MPa)	Tensile strength (MPa)
A1	137.0	32.58	1491	15.939
A2	152.0	36.15	1763	16.147
A3	148.0	35.20	2362	14.969
A4	153.5	36.50	1907	16.476
A5	151.0	35.91	1972	15.731
A6	140.0	33.29	2082	15.315
A7	165.0	39.24	2252	16.182
A8	163.0	38.76	2524	15.714
A9	143.0	34.01	2261	12.821
A10	166.0	39.48	2261	15.956
A11	155.0	36.86	2331	13.877
A12	129.5	30.80	2467	11.0
A13	120.0	28.54	2480	10.9
A14	148.0	35.20	2042	13.5

for 15 min and analyzed by an online linked gas chromatograph/mass spectrometer (GC/MS), an Agilent 6890N15795C GCMSTM (Agilent Co., Ltd., USA) which was linked to a mass selective detector. An elastic quartz capillary column (DB-5MS; 30 m³ 0.25 mm³ 0.25 lm) coated with a neutral phase (Hewlett-Packard-5 cross-linked 5.00% phenyl methyl silicone) was used. The carrier gas was helium and the injection port temperature was 280 °C. The GC temperature program began at 45 °C for 3 min and increased at 8 °C/min until 120 °C, then 20 °C/min until 300 °C was reached and held for 5 min, followed by a split injection at ratio of 30:1. The MS program scanned over a range of 29–500 AMU (*m/z*), at an ionizing voltage of 70 eV. The flow velocity of the He carrier gas was 1.2 mL/min. Ion source temperature: 230 °C, quadrupole temperature 150 °C (Peng et al., 2012).

3. Results and discussion

3.1. Analysis of mechanical properties

The mechanical properties of materials are a main parameter for evaluating materials, and the tensile properties are the most

important criteria in mechanical properties. The mechanical properties of the material generally provide a reliable basis for material selection, structural strength calculation and stiffness. The mechanical properties of the samples were significantly changed after mixing with different proportions of rotten wood flour, CaCO₃, AHP, APP and CaHP. The test results are shown in Table 2. Compared with the samples A2 and A14, with the addition of CaCO₃, the MOR and tensile strength of the composites were obviously improved. During the test, the parallel samples of A2 showed brittle fracture, and the composites showed the characteristics of brittle materials with high strength and low toughness. It can be clearly seen that the addition of CaCO₃ makes the material transition from plastic deformation to brittle deformation. This is due to CaCO₃ can improve the rigidity of the material, limiting the molecular motion, making it into a brittle deformation. In the PBS matrix, CaCO₃ particles play a rigid skeleton role. Compared with the samples A1, A2 and A3, it can be seen that the MOR, MOE and tensile strength of the composites have different trends. Comprehensive considerations, with the increase of wood flour, the composite materials have better comprehensive mechanical properties when the wood powder filling amount of 40 copies. Too much or too little wood will affect the mechanical properties of the composites. This is

mainly due to the fact that wood powder is not easy to disperse, the wood fiber has strong polarity, and it has poor compatibility with PBS resin. The increase of wood powder increases the coagulation phenomenon, and the wood powder particle is concentrated into the stress concentration. In addition, the wood powder as organic filler, low density, the volume fraction of wood powder in the system increases, the relative content of PBS decreases, the load-bearing part decreases, the tensile strength of the composites increases first and then decreases. This is because, Wood powder acts as a dispersing phase and acts as a stress concentration in the matrix, which does not deform by force and does not stop cracks or produce crazing absorption shock energy, thereby increasing the brittleness of the filling system. Thus, the brittleness of the filling system is increased.

Compared with samples A2, A4, A5 and A6, it is observed that when a small amount of AHP is added to the composite, MOR, MOE and tensile strength increased to 36.50 MPa, 1907 MPa and 16.476 MPa. This phenomenon is mainly due to the role of AHP as a flame retardant with inorganic fillers and reinforcing agents. However, adding too much AHP can make the MOR and tensile strength decreased slightly, but with the increase of AHP, the MOE increased continuously. The above phenomenon is mainly caused by the inconsistency between the PBS molecules and the limited compatibility between the AHP particles with the polymer matrix.

Compared with samples A2, A7, A8 and A9, it is observed that when a small amount of APP is added to the composite, MOR, MOE and tensile strength increased to 39.24 MPa, 2252 MPa and 16.182 MPa. Why can appear this kind of phenomenon? The main reason is the APP in the composite cooling crystallization can act as the nucleus, resulting in the formation of the final crystal ball smaller, so that the toughness is improved, MOR, MOE and tensile strength of the composite material will increased. However, The interface between the small number of APP granules and the matrix PBS has a good compatibility, but the mechanical properties of the composites will be decreased with the increase of the amount of APP. This is due to the poor compatibility and non-uniform distribution, between the excessive APP and the polymer matrix, which makes it easy to form stress concentration and become the initiation point for stress destroy. That leads to a decline in mechanical properties.

Compared with samples A2, A10, A11 and A12, it is observed that when a small amount of CaHP is added to the composite, MOR, MOE and tensile strength increased to 39.48 MPa, 2261 MPa and 15.956 MPa. This phenomenon is mainly caused by the fact that CaHP, as a kind of inorganic flame retardants and reinforcing agents can improve the mechanical properties of materials, but the poor interfacial compatibility between the excessive CaHP and PBS, and easy to cause stress concentration, so when adding too much CaHP can lead to the decreased of the mechanical properties.

3.2. Analysis of cone calorimeter

The cone calorimeter is a test method which can effectively detect the combustion behavior of materials under real combustion conditions (Cheng et al., 2012). Figs. 3 and 4, are the heat release rate (HRR) curve and the total heat release (THR) curve of the sample under the condition of the different



Fig. 2 The chemical structure of the PBS model.

flame retardants were added, and the relevant data of the cone calorimeter were summarized in Table 3.

The A14 values of A4, A7, A10, A13 and TTI materials are 36 s, 39 s, 44 s, 44 s, and 44 s, respectively, as indicated in Table 3. The addition of AHP and APP makes the ignition time advance, which is very common in many composites with flame retardants. This is mainly due to the degradation of acidic such as phosphine or small molecule products, which is produced by AHP, and catalyze the degradation of PBS molecular chain. The polymer phosphoric acid produced by APP pyrolysis can catalyze the dehydration reaction of the xylan in the wood fiber and the combustion reaction is easier to be carried out. When adding CaHP, AHP, combination of APP and CaHP three kinds of flame retardants, the ignition time did not change, noted that adding CaHP has no effect on the ignition time of the material. The three kinds of flame retardants of AHP, APP and CaHP were inhibited during decomposition, which leads to the ignition time neither delay nor advance.

Heat release rate (HRR) is one of the important parameters of flame retardant properties. It is well known that the lower the heat release rate in the material combustion process, the better the flame retardant effect of the flame retardants. As shown in Fig. 3, and Table 3, the non-flame retardant composite A14 burns rapidly after 35 kW m⁻² radiation is ignited, the highest peak of heat release rate (pk-HRR) is 332.2 kW·m⁻², the total heat release of wood-plastic composites is 137.8 MJ m⁻². However, the pHRR of composite A4, A7, A10 and A13 decreased obviously after adding flame retardants. Among them, the A13 effect of three kinds of composite materials, such as AHP, APP and CaHP, is the most obvious, and the effect of adding AHP, APP and CaHP separately is weakened in turn. Fig. 3, curve shows that there are two peaks in the composite material, which is mainly caused by the rupture of the carbon layer, which leads to 2 peaks. With the addition of AHP, APP and CaHP, the time of peak heat release rate has been advanced in varying degrees, this is the result of flame retardants promoting PBS thermal degradation, and the heat release rate curve of combustion is further widened. For A4 and A10, there are two distinct peaks of heat release rate, and AHP, CaHP thermal decomposition absorbs the surface heat, reduces the heating temperature of composites, and releases large amounts of water to dilute oxygen on the surface, reducing the peak of the first heat release rate. The degradation of pH₃ produced by the AHP in the first stage, will rapidly react with oxygen in the air to produce H₃PO₄, and

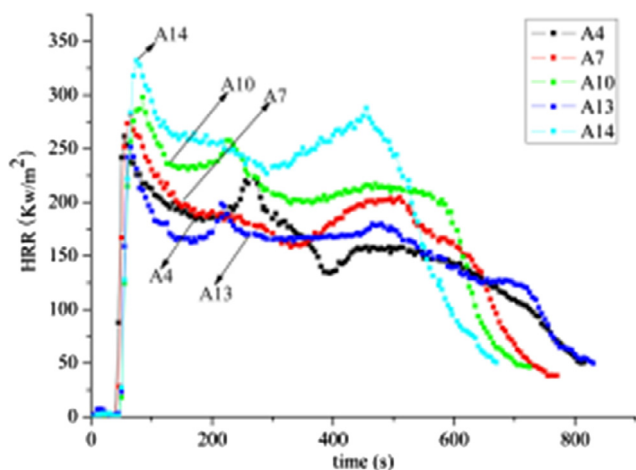


Fig. 3 Heat release rate (HRR) plots for A4, A7, A10, A13 and A14, at a heat flux of 35 kW/m².

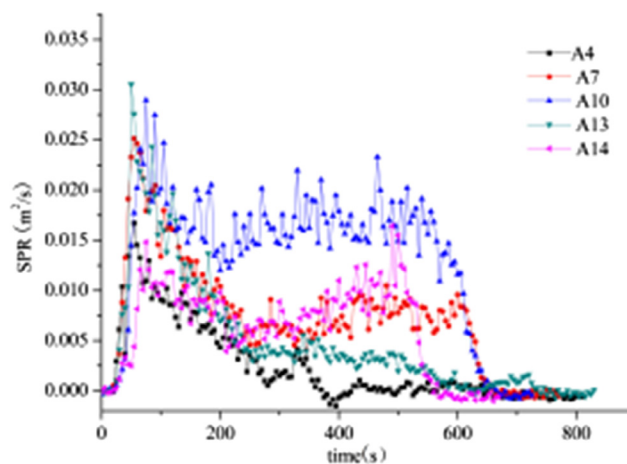


Fig. 5 SPR for A4, A7, A10, A13 and A14, at a heat flux of 35 kW/m².

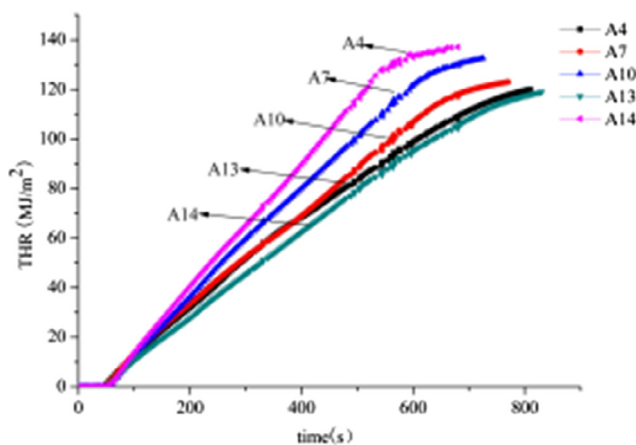


Fig. 4 THR for A4, A7, A10, A13 and A14, at a heat flux of 35 kW/m².

in this process, a large amount of H₃PO₄ exists in coagulation. H₃PO₄ at high temperature will be further condensed to produce poly-phosphoric acid with different degree of polymerization, and also water generated. The H₃PO₄ produced by large amounts of pH₃ oxidation and hypophosphorous acid produced by dehydration can promote PBS to catalyze carbon, to inhibit the complete combustion of PBS molecular chains. The degradation of aluminum hypophosphite produces relatively stable aluminum phosphate and aluminum pyrophosphate at the same. Principle of CaHP degradation of flame

retardant is consistent with AHP, and it is obvious that the flame retardant efficiency of CaHP is slightly lower than AHP. For the A7 system, the APP can produced poly-phosphoric acid at high temperature and can catalyzed some of the PBS and wood fiber into carbon, the carbon layer formed on the surface can protect the following maldi, play the role of insulation, inhibiting material combustion, reducing the rate of heat release. For the A13 system, the pHRR and THR are the smallest of the three kinds of flame retardants, such as AHP, APP and CaHP, which shows that three kinds of flame retardants have synergistic effect on reducing the pHRR and THR.

In the actual fire, more than half of the number is not burned to death, but because of smoke inhalation of toxic smoke suffocated. Therefore, combustible materials in the combustion process, the less the release of smoke, the higher the safety, the greater the probability of escape. From Figs. 5 and 6, and Table 3, can be seen in the A4 system, AHP can effectively reduce the smoke release rate and total smoke generation. However, APP and CaHP cannot effectively reduce the release rate of smoke and the total amount of smoke in A7 and A10 system, but the increase of smoke release rate and total smoke production. In the A13 system, when AHP, APP and CaHP were used in combination with three kinds of flame retardants, the smoke release rate and total smoke production is slightly lower than the A14 system but higher than the A4 system. The main reason for this phenomenon is that AHP has a high smoke suppression effect. The release rate and total smoke generation of A13 system are lower than that of A14 system. However, when AHP, APP and CaHP are used

Table 3 Cone calorimetric test results.

Samples	TTI (S)	pHRR (kW m ⁻²)	THR (MJ/m ²)	Mass (%)	TSP (m ²)	Burning time (s)
A4	36.00	261.55	120.02	20	2.02	823
A7	39.00	282.30	122.95	21	5.65	780
A10	44.00	297.96	132.53	18	9.66	736
A13	44.00	251.58	118.80	27	3.91	840
A14	44.00	332.19	137.83	12	4.26	682

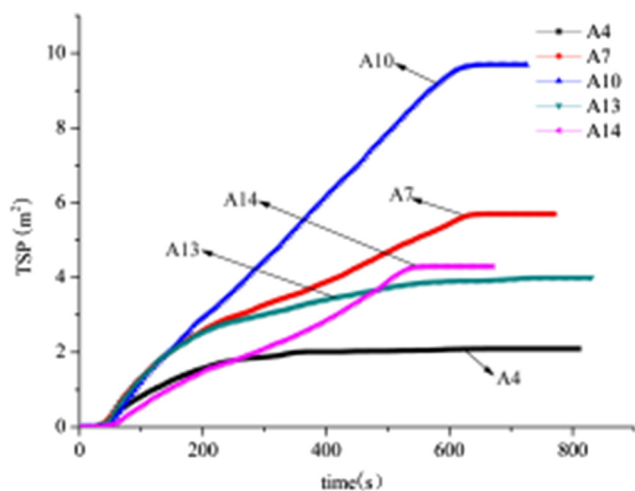


Fig. 6 TSP for A4, A7, A10, A13 and A14, at a heat flux of 35 kW/m².

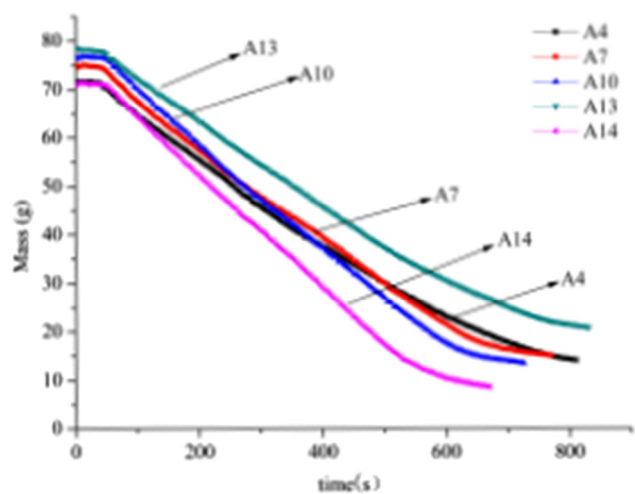


Fig. 7 Mass for A4, A7, A10, A13 and A14, at a heat flux of 35 kW/m².

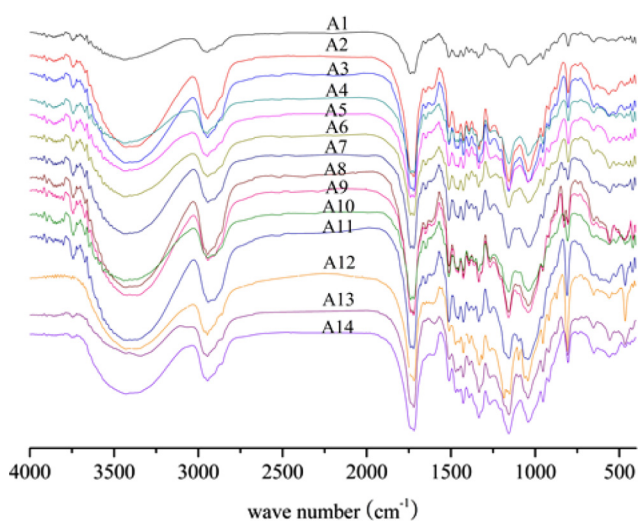


Fig. 8 FT-IR spectra of composites.

in combination, Kinds of flame retardants in the suppression of smoke between the mutual inhibition, thereby reducing the AHP smoke suppression effect. Therefore, the A13 system smoke release rate and total smoke production and slightly higher than the A4 system. In addition, in the A7 system, the initial release rate of APP in the combustion of APP was slightly higher than that of the composite without adding flame retardant, and the release rate of smoke was slightly decreased. Indicating that APP to promote the decomposition of wood fiber dehydration process produced a large number of volatile gases, the formation of carbon and inhibit the composite of the smoke emissions. However, in the combustion process, due to the decomposition of APP to produce ammonia. Not only offset the carbon layer on the inhibition of smoke, but also the rapid increase in the rate of smoke release. The addition of APP improved the total smoke release of the composites.

As can be seen from Fig. 7, and Table 3, the residual carbon content of the sample is as follows: A13, A7, A4, A10, A14. A13 > A7 > A4 > A10 > A14 indicates that the addition of flame retardants to the PBS composite material is better than the thermal stability of the formation of the carbon layer by the combustion of the PBS composite. A7 > A4 > A10 shows that APP has a significant effect on the thermal stability of the reinforced carbon layer, followed by AHP and CaHP. At the same time, AHP, APP and CaHP three kinds of flame retardant compound system used to form the maximum amount of carbon residue.

3.3. Analysis of FT-IR

The broad and medium intensity peak at 955 cm⁻¹ is attributed to -C-OH bending of carboxylic groups in PBS. The stretching vibration of ester carbonyl (>C=O) groups was observed at 1718 cm⁻¹ (Kim and Kim, 2008; Muthuraj et al., 2015). The band at 1041 cm⁻¹ corresponds to the -O-C-C- stretching vibration PBS (Phua et al., 2011). Most of the saturated hydrocarbons contain methyl groups. These methyl and methylene C-H stretching bands at 2954 cm⁻¹ and an asymmetric stretching band 2855 at cm⁻¹ (Cai et al., 2013). In PBS, methyl and methylene C-H stretching bands occur at 2945 and 2855 cm⁻¹, respectively (Liu et al., 2016; Zhang et al., 2015; Song et al., 2008;). The characteristic functional group of ester linkages is -C-O-C-. A strong -C-O-C- stretching peak (1164 cm⁻¹) was observed in PBS, which confirms that the PBS contains ester linkages (Song et al., 2008; Bourbigot et al., 1993).

FT-IR spectra were used to study the structural groups of wood flour and biocomposites. For comparison, the spectra of the fourteen samples listed above are shown in Fig. 8. Peaks at 955, 806 and 644 cm⁻¹ were attributed to C-O stretching, CH₂ in OC(CH₂)₂CO in-plane bending, and -COO bending bands of the PBS (Cai et al., 2013). These peaks are clear evidence to differentiate PBS from other polymers.

All spectra have similar spectral patterns in addition to different intensities of infrared absorption. The main components of wood flour, including cellulose, hemicellulose, lignin, whose infrared spectra is more complex, and the most obvious peak is the stretching vibration absorption peak of 3414 cm⁻¹. The most typical bands (1600, 1510, and 1460 cm⁻¹) are represented aromatic regions of lignin (Wen et al., 2014). The composite has the characteristic peaks of PBS, In the A4, A5, A6

and A13 systems, at 817 cm^{-1} , corresponding to the oscillatory vibration peak of pH_2 and 484 cm^{-1} is the stretching vibration peak of Al—O bond. And the absorption peak of P—O—P appeared at 1100 cm^{-1} , indicating the formation of $\text{Al}_4(\text{P}_2\text{O}_7)_3$ (Yang et al., 2011). In the A10, A11, A12, and A13 systems, 817 cm^{-1} corresponds to the rocking vibration peak of pH_2 , and the characteristic peak in 467 cm^{-1} is the stretching vibration of Ca—O bond. A significant P—O—P characteristic peak appears at 1080 cm^{-1} , indicating the formation of $\text{Ca}_3(\text{PO}_4)_2$ and $\text{Ca}_2\text{P}_2\text{O}_7$.

3.4. Analysis of TG

The thermal stability of polymer materials to a large extent determine its excellent flame retardant properties, therefore, the analysis of thermal stability is also an effective way to evaluate the flame retardancy of polymer materials. In order to further study the effect of AHP, APP, CaHP and CaCO_3 on the thermal stability of PBS, we conducted a TGA test. As shown in Figs. 9 and 10, the Fig. 9, is the TGA curve under air condition, and the Fig. 10, is the DTG curve under air condition. $T_{5\text{wt}\%}$, $T_{50\text{wt}\%}$ and T_{max} , respectively, for weight loss of 5 wt%, 50 wt% and maximum weight loss rate. The specific test results are listed in Table 4. It can be seen from the chart, for A1, A2, A3 system, each group TGA curve is very similar, only one weight loss platform. The curves have a long period of gentle period, and then decreased suddenly between $300\text{ }^\circ\text{C}$ and $460\text{ }^\circ\text{C}$, showing a typical one-step degradation reaction and a maximum heat loss temperature of $410\text{ }^\circ\text{C}$, $407\text{ }^\circ\text{C}$, and $405\text{ }^\circ\text{C}$, respectively. It is known that with the gradual increase in temperature, the decomposition of the composite material is sufficient, the final residual carbon quality is less. According to previous studies on the degradation mechanism of PBS (Chrissafis et al., 2005). PBS decomposition mainly through the following two successive stages: (1) when the decomposition temperature is low, PBS mainly through the elimination of the completion of some segments of the random fracture, during which the quality loss is not large; (2) when the decomposition temperature is high, the fracture of the specific chain segment causes PBS to decompose into smaller molecular units, resulting in a significant reduction in the quality of the system. As shown in Figs. 9 and 10, and Table 4, with the decrease of PBS ratio, $T_{5\text{wt}\%}$, $T_{50\text{wt}\%}$ and $T_{\text{max}2}$ decreased, respectively. Indicating that the increase in the proportion of wood powder will reduce the decomposition temperature of composite materials. Compared with A2 and A14, it was found that the degradation temperature of the composites without adding CaCO_3 was $247\text{ }^\circ\text{C}$, $T_{\text{max}1}$ and $T_{\text{max}2}$ were $216\text{ }^\circ\text{C}$ and $410\text{ }^\circ\text{C}$, respectively. This is mainly due to the fact that PBS is first in the process of heating the ester bond breaks to release small molecules, followed by complete cleavage of the PBS backbone. And because of the poor thermal conductivity of CaCO_3 and the addition of a large number of powders, suppressed the heated after PBS chain segment motion, thereby improving the thermal decomposition temperature of composite materials (Min et al., 2008). And appear $T_{\text{max}1}$, may be due to the composite material without CaCO_3 and other additives, resulting in rapid degradation of wood flour at $216\text{ }^\circ\text{C}$. The initial degradation temperature of the composite material A2 is $274\text{ }^\circ\text{C}$. With the increase of AHP content from 5% to 15%, the initial degradation temperatures of com-

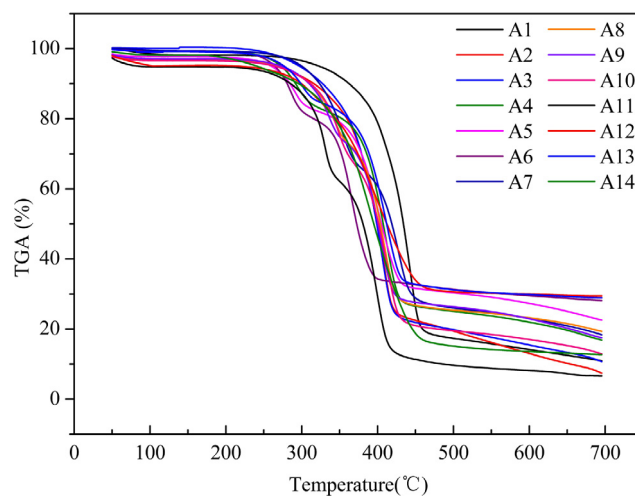
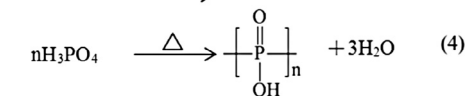
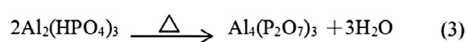
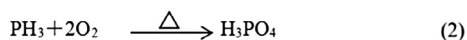
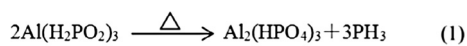


Fig. 9 TGA thermal curves of composites.

posite materials A4, A5 and A6 were $270\text{ }^\circ\text{C}$, $264\text{ }^\circ\text{C}$ and $263\text{ }^\circ\text{C}$. It can be seen that the initial degradation temperature of the composite material is reduced after AHP addition, which is favorable for promoting the formation of wood powder. Because of the composite type containing AHP component of relatively poor stability; At the same time, AHP degradation products can capture free radicals released from wood flour, so that wood powder decomposition time ahead and speed up the wood powder into charcoal. In addition, AHP degradation products may cause degradation of the PBS component. Compared with A1, A2, A3 system, the composite material has only one maximum T_{max} at $407\text{ }^\circ\text{C}$. With the increase of AHP, the composites A4, A5 and A6 had a T_{max} at $400\text{ }^\circ\text{C}$ and $366\text{ }^\circ\text{C}$, and there is a small degradation peak at $292\text{ }^\circ\text{C}$, $291\text{ }^\circ\text{C}$ and $286\text{ }^\circ\text{C}$. This is mainly caused by AHP first degradation process. With the addition of AHP, the content of residual carbon increased from 5% to 14%, 20% and 27% respectively. The degradation of the AHP under air conditions may be carried out as follows:



APP thermal degradation process is divided into two steps, its initial decomposition occurs near $248\text{ }^\circ\text{C}$, releasing H_2O and NH_3 , and the degradation product is highly cross-linked polyphosphoric acid. The second step pyrolysis began in $540\text{ }^\circ\text{C}$, polyphosphoric acid dehydration is decomposed into phosphorus oxide (Fang et al., 2013). Compared with A2, thermal decomposition of A8 and A9 is advanced. This is due to the thermal decomposition products of APP for the cross-linked polyphosphoric acid. It can be used as acid catalyst to promote hemicellulose, cellulose and lignin dehydration. And $T_{5\text{wt}\%}$ and $T_{50\text{wt}\%}$ of A7, increased from $274\text{ }^\circ\text{C}$ and $400\text{ }^\circ\text{C}$ to 303

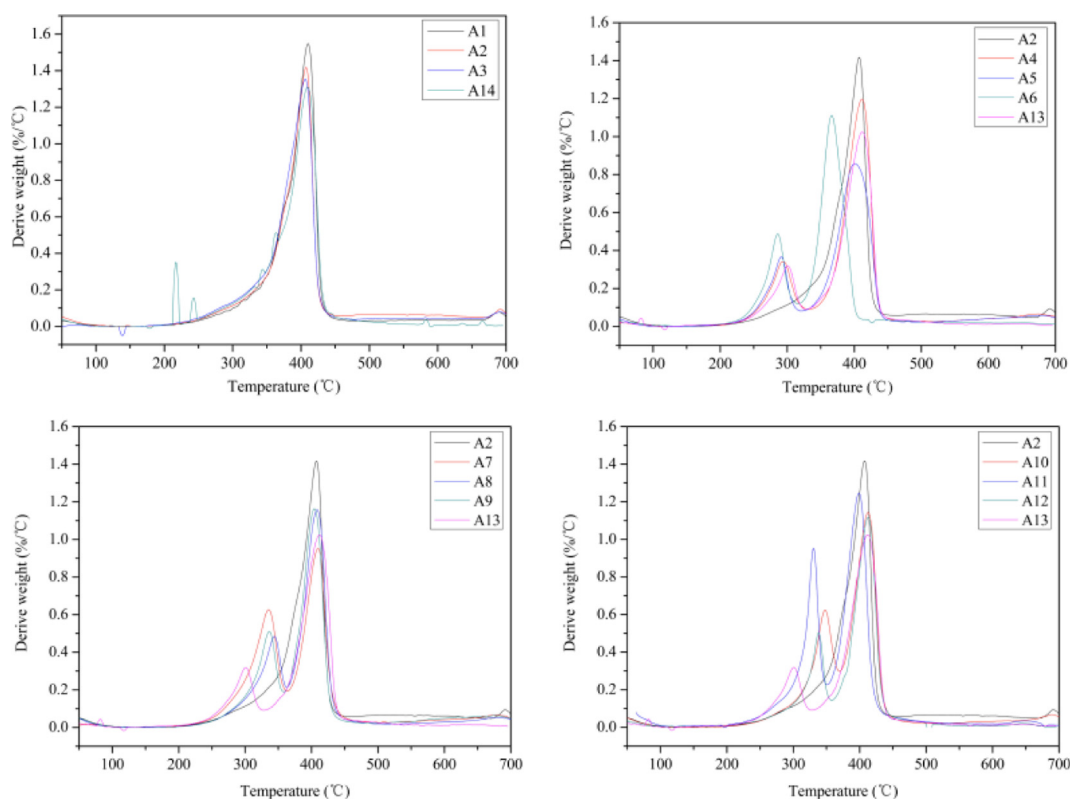


Fig. 10 DTG thermal curves of composites.

Table 4 TGA test results.

Samples	$T_{5wt\%}$ (°C)	$T_{50wt\%}$ (°C)	T_{max1} (°C)	T_{max2} (°C)
A1	329	434		410
A2	274	401		407
A3	268	399		406
A4	276	408	292	411
A5	264	406	291	400
A6	268	374	286	366
A7	303	419	335	409
A8	262	404	344	408
A9	266	401	336	404
A10	273	402	347	412
A11	218	378	330	398
A12	221	413	337	412
A13	280	412	300	410
A14	247	396	216	410

°C and 419 °C, respectively, while APP reduced the maximum weight loss rate. This suggests that a small amount of APP can promote the formation protection of carbon layer, the gas produced by the decomposition of APP can make the carbon layer foam expansion, which play the role of heat insulation, improve material thermal stability. The amount of residual carbon increased to about 17%, shows that by adding flame retardant can greatly improve the system of the residue amount, reduced the amount of flammable gas. Contrast A2, with the increase of CaHP, With the addition of CaHP, the $T_{5wt\%}$, $T_{50wt\%}$ and T_{max} of the composites all decreased first and then increased. This is mainly caused by the dual role of

CaHP, phosphine produced by CaHP decomposition, which can promote the degradation of the chain by PBS. CaHP degradation produces calcium phosphate and calcium pyrophosphate, which can cover the surface of the composite material, effectively prevent the combustion zone heat and material exchange, thus delaying the degradation of PBS. It can also lead to $T_{5wt\%}$, $T_{50wt\%}$ and T_{max} decline; In the oxygen atmosphere, hypophosphorous acid produced by the rapid oxidation of phosphoric acid and phosphoric acid, which can effectively promote the decomposition of PBS into charcoal. This effect can lead to $T_{5wt\%}$ and $T_{50wt\%}$, T_{max} values rise. CaHP content is low, the former factors dominate, CaHP con-

tent high, the latter dominated. With the increase of CaHP, the carbon residue of composites is greatly improved. In addition to the production of calcium phosphate and calcium pyrophosphate, the amount of carbon residue derived from PBS catalyzed charcoal has been significantly improved, indicating that the P from the gas phase to the solid phase and play a catalytic role in the formation of charcoal. Contrast and A4, A7, A10 and A13, there were no apparent different effects between using flame retardants and using one flame retardant. This is mainly due to the three kinds of flame retardants have mutual inhibition in improving the thermal stability of composite materials, which greatly reduces the use of three kinds of flame retardant effect.

3.5. Analysis of XRD

X-ray diffraction can distinguish the crystallization of polymer materials by interfering phenomena, but also distinguish between different crystal forms and the addition of components in the polymer material. The X-ray diffraction pattern of the PBS composite is shown in Fig. 11.

Each sample diffraction pattern shows all three strong diffraction peak, located in the $2\theta = 19.5^\circ$, near 21.9° and 22.6° , respectively, for a crystal of PBS (0 2 0), (0 2 1) and (1 1 0) crystal plane (Dong et al., 2005). The main diffraction peaks of each group were consistent, indicating that the crystal structure of PBS did not change with the increase of AHP, APP and CaHP flame retardants and CaCO_3 . It is worth noting that the intensities of (0 2 0), (0 2 1) and (1 1 0) diffraction peaks decreased with the addition of additives and their contents. This phenomenon can be attributed to AHP, APP, CaHP three kinds of flame retardants and CaCO_3 content of the increase, the crystallization of PBS matrix gradually reduced. This is mainly because with the increase of AHP, APP and CaHP flame retardants and CaCO_3 content, PBS matrix crystallization is also gradually reduced. And AHP, APP, CaHP and CaCO_3 have a certain nucleation effect, improving the nucleation density of PBS matrix. At the same time, AHP, APP, CaHP and CaCO_3 occupy a certain space, ultimately make the spherical crystal growth space is limited and prone to collision, resulting in reduced crystal perfection.

3.6. Analysis of TD-GC-MS

The total ion chromatograms of five kinds of extractives were shown in Figs. 12–16, which were analyzed by GC-MS. And the relative content of each component has been counted by area normalization. The MS data is analyzed by using the NIST standard MS map and publicly published books and papers, and then identify each component.

According to the results of TD-GC-MS analysis, 16 chemical constituents were identified in 37 peaks of A2 volatiles. The results show that the components are: Acetic acid (1.5%, 3.669 min), 1,2-Ethanediol (0.74%, 4.109 min), Furfural (0.74%, 4.109 min), Ethanol, 1-(2-butoxyethoxy)- (0.52%, 11.264 min), 2,2,4-Trimethyl-1,3-pentanediol diisobutyrate (0.73%, 14.084 min), Ethanol, 2-(2-butoxyethoxy)-, acetate (6.65%, 14.259 min), Propanoic acid, 2-methyl-, 3-hydroxy-2,2,4-trimethylpentyl ester (1.79%, 14.427 min), Vanillin (2.14%, 14.886 min), 1H-3a,7-Methanoazulene, 2,3,4,7,8,8a-hexahydro-3,6,8,8-tetramethyl-, [3R-(3.alpha.,3a.beta.,

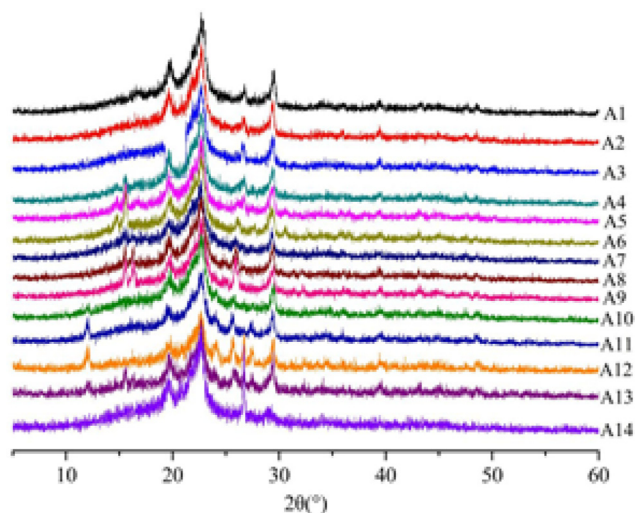


Fig. 11 XRD test result spectrum.

7.beta.,8a.alpha.)]- (1.19%, 15.132 min), Dimethyl phthalate (1.3%, 15.74 min), 1,4-Benzenedicarboxylic acid, dimethyl ester (0.55%, 16.413 min), Benzene, 1,2,3-trimethoxy-5-(2-propenyl)- (1.35%, 17.228 min), 2,2,4-Trimethyl-1,3-pentanediol diisobutyrate (2.9%, 17.862 min), 1,1'-Biphenyl, 2,2',5,5'-tetramethyl- (1.21%, 19.071 min), 1,1'-Biphenyl, 3,4-diethyl- (1.21%, 19.162 min), Phthalic acid, hex-3-yl isobutyl ester (40.71%, 20.164 min).

According to the results of TD-GC-MS analysis, 32 chemical constituents were identified in 75 peaks of A4 volatiles. The results show that the components are: Acetic acid (8.72%, 3.469 min), Dihydroxyacetone (1.05%, 3.896 min), Formamide, N,N-dimethyl- (3.57%, 4.614 min), Furfural (7.95%, 4.685 min), 2(5H)-Furanone (0.53%, 6.373 min), 2-Furancarboxaldehyde, 5-methyl- (0.78%, 6.994 min), Phenol (1.82%, 7.376 min), 1H-Pyrrole-2-carboxaldehyde (2.72%, 8.029 min), Dihydro-3-methylene-5-methyl-2-furanone (0.86%, 9.161 min), Nonanal (0.52%, 9.608 min), Ethanol, 2-(2-butoxyethoxy)- (2.22%, 11.218 min), 2,2,4-Trimethyl-1,3-pentanediol diisobutyrate (3.04%, 14.065 min), Ethanol, 2-(2-butoxyethoxy)-, acetate (15.9%, 14.233 min), Propanoic acid, 2-methyl-, 3-hydroxy-2,2,4-trimethylpentyl ester (5.4%, 14.414 min), Vanillin (6.66%, 14.847 min), Dimethyl phthalate (3.14%, 15.708 min), 1,4-Benzenedicarboxylic acid, dimethyl ester (0.96%, 16.393 min), 2,4-Di-tert-butylphenol (1.44%, 16.536 min), Butylated Hydroxytoluene (0.58%, 16.594 min), Benzene, 1,2,3-trimethoxy-5-(2-propenyl)- (3.46%, 17.208 min), 2,2,4-Trimethyl-1,3-pentanediol diisobutyrate (13.44%, 17.855 min), Cedrol (3.81%, 18.062 min), 1,1'-Biphenyl, 2,2',5,5'-tetramethyl- (3.58%, 19.065 min), 1,1'-Biphenyl, 3,4-diethyl- (3.69%, 19.155 min), 1,2-Benzenedicarboxylic acid, bis(2-methylpropyl) ester (100%, 21.614 min), Phthalic acid, butyl isohexyl ester (4.86%, 22.112 min), Hexadecanoic acid, methyl ester (12.66%, 22.183 min), 7,9-Di-tert-butyl-1-oxaspiro(4,5)deca-6,9-diene-2,8-dione (12.76%, 22.228 min), Dibutyl phthalate (11.19%, 22.694 min), Phenol, 4-methyl-2-[5-(2-thienyl)pyrazol-3-yl]- (98.6%, 25.592 min), 9-Octadecenamide, (Z)- (11.14%, 27.112 min), 3,3',4,4'-Tetramethoxystilbene (42.11%, 27.552 min).

According to the results of TD-GC-MS analysis, 30 chemical constituents were identified in 62 peaks of A7 volatiles.

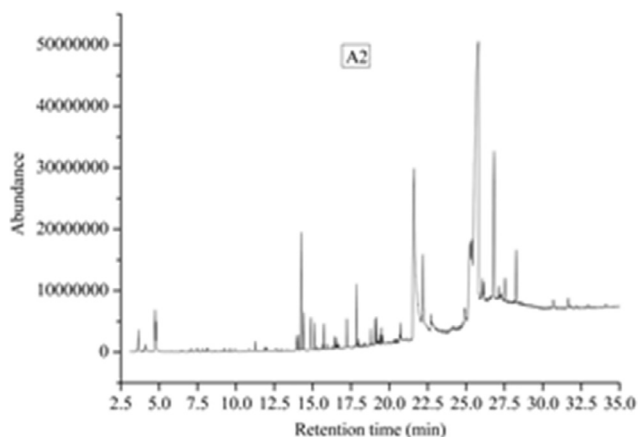


Fig. 12 Total ion chromatogram of A2 composites.

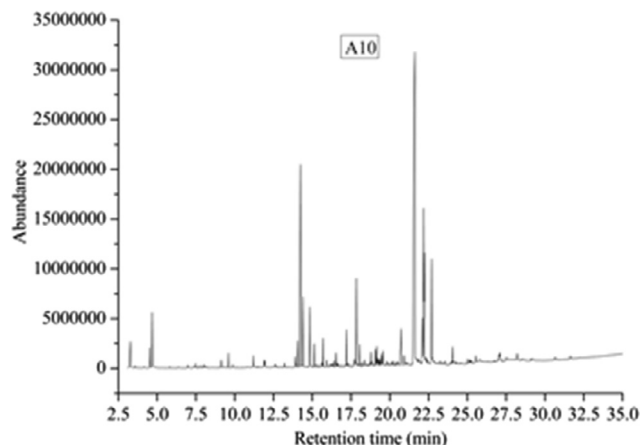


Fig. 15 Total ion chromatogram of A10 composites.

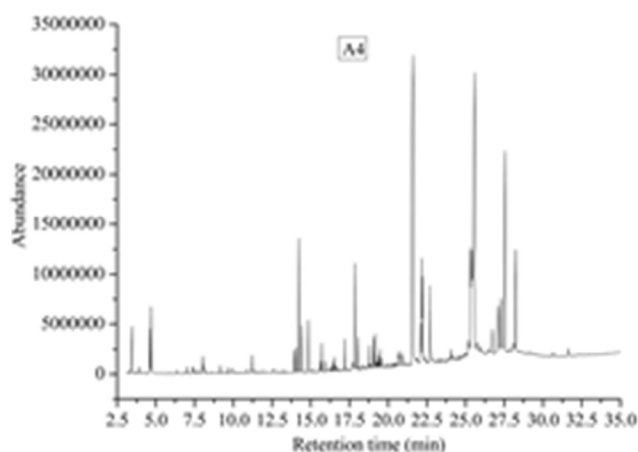


Fig. 13 Total ion chromatogram of A4 composites.

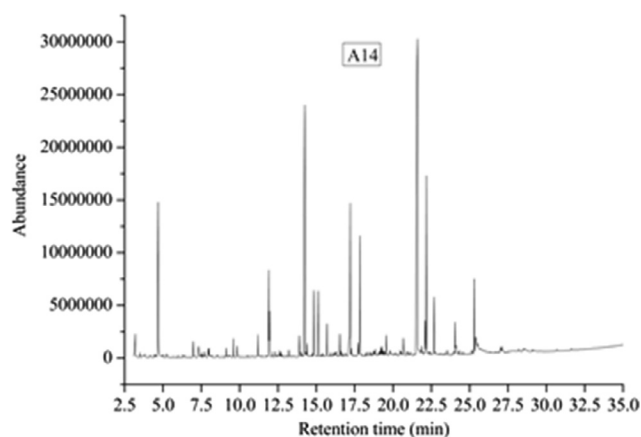


Fig. 16 Total ion chromatogram of A14 composites.

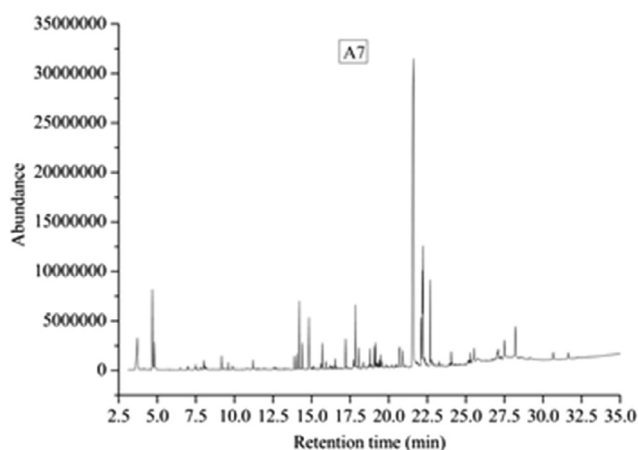


Fig. 14 Total ion chromatogram of A7 composites.

The results show that the components are: Acetic acid (8.39%, 3.708 min), Furfural (8.15%, 4.679 min), Formamide, N,N-dimethyl- (3.56%, 4.801 min), 2-Furancarboxaldehyde, 5-methyl- (0.65%, 6.988 min), 2,7-Dioxatricyclo[4.4.0.0(3,8)]deca-4-ene (0.89%, 7.486 min), 1H-Pyrrole-2-carboxaldehyde (1.52%, 8.016 min), Dihydro-3-methylene-5-methyl-2-fura-

none (1.66%, 9.161 min), Nonanal (0.7%, 9.608 min), Ethanol, 2-(2-butoxyethoxy)- (1.32%, 11.199 min), 2,2,4-Trimethyl-1,3-pentanediol diisobutyrate (1.81%, 14.058 min), Ethanol, 2-(2-butoxyethoxy)-, acetate (7.39%, 14.207 min), Propanoic acid, 2-methyl-, 3-hydroxy-2,2,4-trimethylpentyl ester (2.84%, 14.401 min), Vanillin (6.25%, 14.828 min), Dimethyl phthalate (2.94%, 15.695 min), 2,4-Di-*tert*-butylphenol (1.08%, 16.529 min), Benzene, 1,2,3-trimethoxy-5-(2-propenyl)- (3.2%, 17.196 min), 2,2,4-Trimethyl-1,3-pentanediol diisobutyrate (7.5%, 17.842 min), Cedrol (2.17%, 18.049 min), 1,1'-Biphenyl, 2,2',5,5'-tetramethyl- (2.41%, 19.059 min), 1,1'-Biphenyl, 3,4-diethyl- (2.7%, 19.149 min), Tetradecane, 2,6,10-trimethyl- (0.57%, 19.291 min), 1,1'-Biphenyl, 2,2',5,5'-tetramethyl- (1.75%, 19.466 min), 1,2-Benzenedicarboxylic acid, bis(2-methylpropyl) ester (100%, 21.607 min), Phthalic acid, butyl hex-3-yl ester (5.47%, 22.105 min), Hexadecanoic acid, methyl ester (11.3%, 22.17 min), 7,9-Di-*tert*-butyl-1-oxaspiro(4,5)deca-6,9-diene-2,8-dione (14.87%, 22.228 min), 7,9-Di-*tert*-butyl-1-oxaspiro(4,5)deca-6,9-diene-2,8-dione (0.99%, 22.306 min), Dibutyl phthalate (9.57%, 22.688 min), 1,2-Benzenedicarboxylic acid, butyl octyl ester (1.3%, 22.759 min), 2-Methyl-E,E-3,13-octadecadien-1-ol (1.42%, 24.052 min).

According to the results of TD-GC-MS analysis, 32 chemical constituents were identified in 61 peaks of A10 volatiles.

The results show that the components are: Acetic acid (3.98%, 3.275 min), Formamide, N,N-dimethyl- (1.9%, 4.51 min), Furfural (6.1%, 4.672 min), Dihydro-3-methylene-5-methyl-2-furanone (0.86%, 9.135 min), Nonanal (1.32%, 9.601 min), Ethanol, 2-(2-butoxyethoxy)- (1.52%, 11.199 min), 2-Hexene, 3,4,4-trimethyl- (0.76%, 11.943 min), 2,2,4-Trimethyl-1,3-pentanediol diisobutyrate (2.92%, 14.058 min), Ethanol, 2-(2-butoxyethoxy)-, acetate (27.5%, 14.239 min), ropanoic acid, 2-methyl-, 3-hydroxy-2,2,4-trimethylpentyl ester (7.68%, 14.407 min), Vanillin (6.99%, 14.834 min), 1H-3a,7-Methanoazulene, 2,3,4,7,8,8a-hexahydro-3,6,8,8-tetramethyl-, [3R-(3.alpha.,3a.beta.,7.beta.,8a.alpha.)]- (2.41%, 15.125 min), Dimethyl phthalate (2.91%, 15.695 min), 1,4-Benzenedicarboxylic acid, dimethyl ester (0.6%, 16.387 min), 2,4-Di-*tert*-butylphenol (1.37%, 16.529 min), Benzene, 1,2,3-trimethoxy-5-(2-propenyl)- (3.62%, 17.202 min), 2,2,4-Trimethyl-1,3-pentanediol diisobutyrate (10.77%, 17.849 min), Cedrol (2.38%, 18.049 min), 1,1'-Biphenyl, 2,2',5,5'-tetramethyl- (1.8%, 19.058 min), 1,1'-Biphenyl, 3,4-diethyl- (1.96%, 19.149 min), Tetradecane, 2,6,10-trimethyl- (0.73%, 19.285 min), 1,1'-Biphenyl, 2, 2',5,5'-tetramethyl- (1.57%, 19.466 min), Methyl tetradecanoate (1.29%, 19.556 min), 1-Heptatriacotanol (0.61%, 21.161 min), 1,2-Benzenedicarboxylic acid, bis(2-methylpropyl) ester (100%, 21.614 min), Phthalic acid, butyl hex-3-yl ester (5.15%, 22.112 min), Hexadecanoic acid, methyl ester (17.62%, 22.183 min), 7,9-Di-*tert*-butyl-1-oxaspiro(4,5)deca-6,9-diene-2,8-dione (12.62%, 22.228 min), 7,9-Di-*tert*-butyl-1-oxaspiro(4,5)deca-6,9-diene-2,8-dione (0.76%, 22.312 min), Dibutyl phthalate (12.42%, 22.694 min), 2-Methyl-E,E-3,13-octadecadien-1-ol (1.94%, 24.052 min), 1H-2,8a-Methanocyclopenta[a]cyclopropa[e]cyclodecen-11-one, 1a,2,5,5a,6,9,10,10a-octahydro-5,5a,6-trihydroxy-1,4-bis(hydroxymethyl)-1,7,9-trimethyl-, [1S-(1.alpha.,1a.alpha.,2.alpha.,5.beta.,5a.beta.,6.beta.,8a.alpha.,9.alpha.,10a.alpha.)]- (0.64%, 24.117 min).

According to the results of TD-GC-MS analysis, 41 chemical constituents were identified in 67 peaks of A14 volatiles. The results show that the components are: Acetic acid (3.97%, 3.197 min), Furfural (23.32%, 4.691 min), 2,4-Hexadiene, 2,5-dimethyl- (0.69%, 5.248 min), 2-Furancarboxaldehyde, 5-methyl- (2.19%, 6.975 min), Phenol (2.46%, 7.318 min), Cyclotetrasiloxane, octamethyl- (0.56%, 7.576 min), 1H-Pyrrole-2-carboxaldehyde (1%, 7.952 min), 2-Cyclopenten-1-one, 2-hydroxy-3-methyl- (1.4%, 7.997 min), Dihydro-3-methylene-5-methyl-2-furanone (9.122%, 1.15 min), Nonanal (1.9%, 9.595 min), Ethanol, 2-(2-butoxyethoxy)- (2.78%, 11.192 min), 3,4-Dimethylcyclohexanol (9.3%, 11.904 min), Sulfurous acid, cyclohexylmethyl nonyl ester (5.01%, 11.949 min), Cyclopropanemethanol, 2,2,3,3-tetramethyl- (0.61%, 12.344 min), Benzeneacetaldehyde, .alpha.-ethyl- (0.52%, 12.693 min), Formamide, N,N-dibutyl- (0.82%, 13.204 min), Ethanol, 2-(2-butoxyethoxy)-, acetate (44.53%, 14.246 min), Propanoic acid, 2-methyl-, 3-hydroxy-2,2,4-trimethylpentyl ester (1.67%, 14.394 min), Vanillin (8.7%, 14.834 min), 1H-3a,7-Methanoazulene, 2,3,4,7,8,8a-hexahydro-3,6,8,8-tetramethyl-, [3R-(3.alpha.,3a.beta.,7.beta.,8a.alpha.)]- (7.44%, 15.125 min), Dimethyl phthalate (3.85%, 15.695 min), 2,4-Di-*tert*-butylphenol (2.43%, 16.536 min), Butylated Hydroxytoluene (0.57%, 16.594 min), Benzene, 1,2,3-trimethoxy-5-(2-propenyl)- (23.09%, 17.215 min), 4'-Hydroxy-3'-methoxyaceto

phenone, isopropyl ether (1.72%, 17.719 min), 2,2,4-Trimethyl-1,3-pentanediol diisobutyrate (15.24%, 17.849 min), 1,3,5-Triazine-2,4,6(1H,3H,5H)-trione, 1,3,5-tri-2-propenyl- (0.63%, 18.838 min), 1,1'-Biphenyl, 3,4-diethyl- (0.56%, 19.143 min), Tetradecane, 2,6,10-trimethyl- (0.86%, 19.201 min), Tetradecane, 2,6,10-trimethyl- (1.26%, 19.285 min), Methyl tetradecanoate (2.38%, 19.557 min), Tetradecane, 2,6,10-trimethyl- (2.46%, 20.676 min), 1,2-Benzenedicarboxylic acid, bis(2-methylpropyl) ester (100%, 21.594 min), Phthalic acid, butyl hex-3-yl ester 3.83%, 22.099 min), Hexadecanoic acid, methyl ester (21.42%, 22.176 min), Dibutyl phthalate (6.83%, 22.681 min), 1H-2,8a-Methanocyclopenta[a]cyclopropa[e]cyclodecen-11-one, 1a,2,5,5a,6,9,10,10a-octahydro-5,5a,6-trihydroxy-1,4-bis(hydroxymethyl)-1,7,9-trimethyl-, [1S-(1.alpha.,1a.alpha.,2.alpha.,5.beta.,5a.beta.,6.beta.,8a.alpha.,9.alpha.,10a.alpha.)]- (0.62%, 23.988 min), Oleanitrile (3.64%, 24.052 min), 2-Methyl-E,E-3,13-octadecadien-1-ol (1.34%, 24.098 min), Butyl citrate (8.24%, 25.294 min), Butyl citrate (1.96%, 25.391 min).

It is suggested that the 120 °C volatiles of PBS composite included acetic acid, phenol and its derivatives, and benzene and its derivatives, which could inhibit fungal growth. But phenol, benzene, and their derivatives are toxic. In addition, there was vanillin (2.14%) in the A2 sample, vanillin (6.66%) and cedrol (3.81%) in the A4 sample, vanillin (6.25%) and cedrol (2.17%) in the A7 sample, vanillin (6.99%) in the A10 sample, vanillin (8.7%) in the A14 sample. These contents resulted in the fragrant smell of the PBS composite. The results of TD-GC-MS show that there are many hydrocarbon compounds and lipid compounds in PBS composites, and the toxic components are few. Therefore, PBS composite material is a relatively new type of green composite materials.

4. Conclusions

From the above studies, it can be seen that CaCO₃ can enhance the tensile strength of the composites, and the toughness decreases. In this study, Too much or too little wood flour will also affect the mechanical properties of the composites. Comprehensive considerations, with the increase of wood flour, the composite materials have better comprehensive mechanical properties when the wood powder filling amount of 40 copies. A small amount of AHP, APP and CaHP can enhance the mechanical properties of the composites. It is well known that the lower the heat release rate in the material combustion process, the better the flame retardant effect of the flame retardants. When the AHP, APP and CaHP are used, the flame retardant effect of composite materials is the best, the total heat release is the lowest, the smoke release is the least, and the amount of residual carbon is the most. And the addition of AHP, APP and CaHP can significantly improve the crystallinity of the composites and improve the crystallinity of the composites.

TG test showed that AHP could effectively form the acid source of catalyzed charcoal under air condition. CaHP has better thermal stability than AHP in air condition, and its air conditions are more favorable for CaHP to catalyze the flame retardancy. The addition of APP can effectively improve the amount of the composite material at high temperature, and improve the stability of the system at high temperature. There-

fore, the performance of PBS composite materials is excellent and has a better use prospect.

Acknowledgments

This research was supported by the Planned Science and Technology Project of Hunan Province, China (No. 2016SK2089; No. 2016RS2011), Major Scientific and Technological Achievements Transformation Projects of Strategic Emerging Industries in Hunan Province (2016GK4045), Academician reserve personnel training plan of lift engineering technical personnel of Hunan Science and Technology Association (2017TJ-Y10).

References

- Ayrlimis, N., Jarusombuti, S., 2010. Flat-pressed wood plastic composite as an alternative to conventional wood-based panels. *J. Compos. Mater.* 45 (1), 103–112.
- Aziz, N.I.H.A., Hanafiah, M.M., 2017. The Potential of Palm Oil Mill Effluent (POME) as a renewable energy source. *Acta Sci. Malaysia* 1 (2), 09–11.
- Basheer, A.O., Hanafiah, M.M., Abdulhasan, M.J., 2017. A Study on Water Quality from Langat River. Selangor. *Acta Scientifica Malaysia* 1 (2), 01–04.
- Bourbigot, S., Bras, M.L., Delobel, R., 1993. Carbonization mechanisms resulting from intumescence association with the ammonium polyphosphate-pentaerythritol fire retardant system. *Carbon* 31 (8), 1219–1230.
- Cai, Y., Lv, J., Feng, J., 2013. Spectral characterization of four kinds of biodegradable plastics: poly (lactic acid), poly (butylenes adipate-co-terephthalate), poly (hydroxybutyrate-co-hydroxyvalerate) and poly (butylenes succinate) with ftir and raman spectroscopy. *J. Polym. Environ.* 21 (1), 108–114.
- Cheng, K.C., Yu, C.B., Guo, W., Wang, S.F., Chuang, T.H., Lin, Y. H., 2012. Thermal properties and flammability of polylactide nanocomposites with aluminum trihydrate and organoclay. *Carbohydr. Polym.* 87 (2), 1119–1123.
- Chrissafis, K., Paraskevopoulos, K.M., Bikiaris, D.N., 2005. Thermal degradation mechanism of poly(ethylene succinate) and poly (butylene succinate): comparative study. *Thermochim. Acta.* 435 (2), 142–150.
- Dash, B.N., Nakamura, M., Sahoo, S., Kotaki, M., Nakai, A., Hamada, H., 2008. Mechanical properties of hemp reinforced poly (butylene succinate) biocomposites. *J. Biobased. Mater. Bio.* 2 (3), 273–281 (9).
- Deschamps, A.A., Grijpma, D.W., Feijen, J., 2001. Poly(ethylene oxide)/poly(butylene terephthalate) segmented block copolymers: the effect of copolymer composition on physical properties and degradation behavior. *Polymer* 42 (23), 9335–9345.
- Dicker, M.P.M., Duckworth, P.F., Baker, A.B., Francois, G., Hazard, M.K., Weaver, P.M., 2014. Green composites: a review of material attributes and complementary applications. *Compos. Part. A – Appl. Sci.* 56 (1), 280–289.
- Dong, T., He, Y., Zhu, B., Kyungmoo Shin, A., Inoue, Y., 2005. Nucleation mechanism of α -cyclodextrin-enhanced crystallization of some semicrystalline aliphatic polymers. *Macromolecules* 38 (18), 7736–7744.
- Fang, Y., Wang, Q., Guo, C., Song, Y., Cooper, P.A., 2013. Effect of zinc borate and wood flour on thermal degradation and fire retardancy of polyvinyl chloride (PVC) composites. *J. Anal. Appl. Pyrol.* 100 (100), 230–236.
- Gamon, G., Evon, P., Rigal, L., 2013. Twin-screw extrusion impact on natural fibre morphology and material properties in poly(lactic acid) based biocomposites. *Ind. Crops. Prod.* 46 (4), 173–185.
- Gann, R.G., Babrauskas, V., Peacock Jr., R.D., Hall, J.R., 2010. Fire conditions for smoke toxicity measurement. *Fire. Mater.* 18 (3), 193–199.
- Ghafar, F., Nazrin, T.N.N.T., Salleh, M.R.M., Hadi, N.N., Ahmad, N., Hamzah, A.A., Yusof, Z.A.M., Azman, I.N., 2017. Total phenolic content and total flavonoid content in moringa oleifera seed. *Sci. Heritage J.* 1 (1), 23–25.
- Halim, H., Abdullah, R., Nor, M.J.M., Aziz, H.A., Rahman, N.A., 2017. Comparison between measured traffic noise in Klang valley, Malaysia and existing prediction models. *Eng. Heritage J.* 1 (2), 10–14.
- Halim, N.I.A., Phang, I.C., 2017. Salicylic acid mitigates Pb stress in *Nicotiana tabacum*. *Sci. Heritage J.* 1 (1), 16–19.
- Hassan, S.R., Zaman, N.Q., Dahlan, I., 2017. Influence of seed loads on start up of modified anaerobic hybrid baffled (MAHB) reactor treating recycled paper wastewater. *Eng. Heritage J.* 1 (2), 05–09.
- Ismail, H., Hanafiah, M.M., 2017. Management of end-of-life electrical and electronic products: the challenges and the potential solutions for management enhancement in developing countries context. *Acta Sci. Malaysia* 1 (2), 05–08.
- Jiang, S.C., Ge, S.B., Wu, X., Yang, Y.M., Chen, J.T., Peng, W.X., 2017. Treating n-butane by activated carbon and metal oxides. *Toxicol. Environ. Chem.*, 1–12.
- Khan, I.U., Sajid, S., Javed, A., Sajid, S., Shah, S.U., Khan, S.N., Ullah, K., 2017. Comparative diagnosis of typhoid fever by polymerase chain reaction and widal test in southern districts (Bannu, Lakki Marwat And D.I. Khan) of Khyber Pakhtunkhwa, Pakistan. *Acta Sci. Malaysia* 1 (2), 12–15.
- Kim, H.S., Kim, H.J., 2008. Enhanced hydrolysis resistance of biodegradable polymers and bio-composites. *Polym. Degrad. Stab.* 93 (8), 1544–1553.
- Koronis, G., Silva, A., Fontul, M., 2013. Erratum to “‘corrigendum to ‘green composites: a review of adequate materials for automotive applications’ [composites part b: engineering 44 (2013) 120–127]” [composites part b: engineering 47 (2013) 391]. *Compos. Part. B – Eng.* 49 (1), 120–127.
- Kutláková, K.M., Tokarský, J., Kovář, P., Vojtěšková, S., Kovářová, A., Smetana, B., Kukutschová, J., Čapková, P., Matějka, V., 2011. Preparation and characterization of photoactive composite kaolinite/TiO₂. *J. Hazard. Mater.* 188 (1–3), 212–220.
- Liu, L., Qian, M., Song, P., Huang, G., Yu, Y., Fu, S., 2016. Fabrication of green lignin-based flame retardants for enhancing the thermal and fire retardancy properties of polypropylene/wood composites. *ACS Sustain Chem. Eng.* 4 (4).
- Mantia, F.P.L., Morreale, M., 2011. Green composites: a brief review. *Compos. Part. A – Appl. Sci.* 42 (6), 579–588.
- Min, W.L., Han, S.O., Seo, Y.B., 2008. Red algae fibre/poly(butylene succinate) biocomposites: the effect of fibre content on their mechanical and thermal properties. *Compos. Sci. Technol.* 68 (6), 1266–1272.
- Muthuraj, R., Misra, M., Mohanty, A.K., 2015. Hydrolytic degradation of biodegradable polyesters under simulated environmental conditions. *J. Appl. Polym. Sci.* 132, 42189–42201.
- Peng, W.X., Wang, L.S., Xu, Q., Wu, Q.D., Xiang, S.L., 2012. TD-GC-MS analysis on thermal release behavior of poplar composite biomaterial under high temperature. *J. Comput. Theor. Nanos.* 9 (9), 1431–1433.
- Peng, W.X., Wang, L.S., Zhang, M.L., Lin, Z., 2013. Molecule characteristics of eucalyptus hemicelluloses for medical microbiology. *J. Pure. Appl. Microbio.* 7 (2), 1345–1349.
- Peng, W.X., Xue, Q., Ohkoshi, M., 2014. Immune effects of extractives on bamboo biomass self-plasticization. *Pak. J. Pharm. Sci.* 27 (4 Suppl), 991–999.
- Phua, Y.J., Chow, W.S., Ishak, Z.A.M., 2011. The hydrolytic effect of moisture and hygrothermal aging on poly(butylene succinate)/organo-montmorillonite nanocomposites. *Polym. Degrad. Stab.* 96 (7), 1194–1203.

- Prasannalakshmi, P., Shanmugam, N., Kannadasan, N., Sathishkumar, K., Viruthagiri, G., Poonguzhali, R., 2015. Influence of thermal annealing on the photo catalytic properties of TiO₂ nanoparticles under solar irradiation. *J. Mater. Sci-Mater. El.* 26 (10), 7987–7996.
- Rahman, N.A., Halim, H., Gotoh, H., Harada, E., 2017. Validation of microscopic dynamics of grouping pedestrians behavior: from observation to modeling and simulation. *Eng. Heritage J.* 1 (2), 15–18.
- Rath, S.K., Patri, M., Khakhar, D.V., 2012. Structure–thermomechanical property correlation of moisture cured poly(urethane-urea)/clay nanocomposite coatings. *Prog. Org. Coat.* 75 (3), 264–273.
- Razali, M.A.A., Said, F.M., 2017. Red pigment production by *monascus purpureus* in stirred-drum bioreactor. *Sci. Heritage J.* 1 (1), 13–15.
- Schartel, B., Hull, T.R., 2010. Development of fire-retarded materials—interpretation of cone calorimeter data. *Fire. Mater.* 31 (5), 327–354.
- Shamsudin, N.H., Wong, C.H., Rahman, R.N.Z.R.A., Ali, M.S.M., 2017. Tight repression of elastase strain K overexpression by Pt7 (A1/O4/O3) shuttle expression system. *Sci. Heritage J.* 1 (1), 20–22.
- Song, P., Fang, Z., Tong, L., Jin, Y., Lu, F., 2008. Effects of metal chelates on a novel oligomeric intumescent flame retardant system for polypropylene. *J. Anal. Appl. Pyrol.* 82 (2), 286–291.
- Sukor, N.S.A., Jarani, N., Faisal, S.F.M., 2017. Analysis of passengers' access and egress characteristics to the train station. *Eng. Heritage J.* 1 (2), 01–04.
- Wen, J.L., Sun, S.L., Yuan, T.Q., Xu, F., Sun, R.C., 2014. Understanding the chemical and structural transformations of lignin macromolecule during torrefaction. *Appl. Energy* 121 (10), 1–9.
- Xue, Q., Peng, W.X., Ohkoshi, M., 2014. Molecular bonding characteristics of Self-plasticized bamboo composites. *Pak. J. Pharm. Sci.* 27 (4 Suppl), 975.
- Yang, L., Feng, W., Ye, J., 2008. Experimental research on the spatial distribution of toxic gases in the transport of fire smoke. *J. Fire. Sci.* 26 (1), 45–62.
- Yang, W., Hu, Y., Tai, Q., Lu, H., Song, L., Yuen, R.K.K., 2011. Fire and mechanical performance of nanoclay reinforced glass-fiber/PBT composites containing aluminum hypophosphite particles. *Compos. Part A – Appl. Sci.* 42 (7), 794–800.
- Zhang, Y., Li, X., Cao, Z., Fang, Z., Hull, T.R., Stec, A.A., 2015. Synthesis of zinc phosphonated poly(ethylene imine) and its fire retardant effect in low density polyethylene. *Ind. Eng. Chem. Res.* 54 (13), 3247–3256.
- Zini, E., Scandola, M., 2011. Green composites: an overview. *Pol. Ym. Compos.* 32 (12), 1905–1915.